ADDITIVE FABRICATION OF POLYMER-CERAMIC COMPOSITE FOR BONE TISSUE ENGINEERING

S. Ramesh[*], M. Eldakroury*, I.V. Rivero*, M.C. Frank*

[*]Industrial and Manufacturing Systems Engineering, Iowa State University, Ames, IA 50011

Abstract

The objective of this study is to manufacture chitosan-based biocomposite 3-D scaffolds through additive fabrication for promoting the regeneration of bone defects. Additive manufacturing has enabled the production of effective scaffolds by overcoming traditional limitations such as suboptimal distribution of cells, and poor control over scaffold architecture. In this study, cryomilled biocomposites comprising of poly (lactic) acid (PLA), chitosan (CS) and tricalcium phosphate (TCP) provided the basis for the generation of hydrogels, which were then utilized for the fabrication of scaffolds with orthogonal (0, 90) geometry. Rheological studies were conducted using a rotational rheometer to identify the ideal hydrogel concentration for the continuous production of scaffolds. The scaffolds were fabricated using a 3-axis computerized numerical control (CNC) which was modified to function as a customized bioplotter. Scanning electron microscopy (SEM) was used to observe the morphology of the bioplotted scaffolds. Finally, a short-term stability (14 days) study was conducted to analyze the *in vitro* degradation behavior of the scaffolds in phosphate buffer saline (PBS).

Keywords: Bioplotting, Chitosan, Cryomilling, Additive Fabrication, Bone Tissue Engineering

1. Introduction

Bone grafting is a surgical procedure that is frequently implemented to improve bone regeneration in a broad array of orthopedic procedures. Even though autografts are still considered the 'gold standard' for bone-grafting, extracting autologous bone tissue demands supplemental surgery and comes with limitations such as patient inconvenience, insufficient supply, and excessive costs [1]. Thus, conquering these limitations is essential to the development of efficient regenerative techniques to treat bone defects. Over the last few decades, the scaffold-based therapy has emerged as an interesting alternative to overcome challenges associated with traditional tissue transplantation [2]. Natural and synthetic biodegradable polymers have been individually, or in a blended form, for the fabrication of scaffolds, the supportive structure that induces the regeneration of bone tissue [3]. Nevertheless, there is always an opportunity to explore new material combinations in an attempt to fabricate better scaffolds.

Apart from desirable material properties, the design and fabrication of scaffolds have an impact on the success of the treatment. Traditional fabrication techniques such as solvent casting, fiber bonding, and freeze drying provide good macroscale features but often fail to match the complexity of natural human tissue [4]. This necessitates the use of manufacturing techniques that would enable the production of scaffolds satisfying patient-specific needs.

In an attempt to address the above-mentioned aspects, this study presents a preliminary feasibility report on the additive fabrication of 3D scaffolds using a novel biodegradable composite

composed of poly (lactic acid) (PLA), chitosan (CS) and tricalcium phosphate (TCP). PLA, a synthetic polyester is known for its biocompatibility and suitable mechanical properties, however, the release of acid by-products during its hydrolytic degradation *in vivo* may have undesirable effects [5]. Likewise, CS, a naturally occurring polysaccharide, also possesses both desirable and undesirable qualities. It is used in the fabrication of biomedical scaffolds by virtue of its antimicrobial and biodegradable properties. However, its inappropriate mechanical and degradation properties have limited its exclusive use for medical applications [6]. The benefit of including TCP into a polymer matrix is twofold (a) it enhances material strength (b) also ensures the maintenance of a suitable ionic environment by neutralizing the acidic degradation of polyesters [5]. Taking together all these observations, it was hypothesized that the fabrication of biocomposite scaffold comprised of PLA, CS and TCP would be an effective solution to conceal the inherent drawbacks of these materials.

In this study, additive fabrication was utilized for the fabrication of biocomposite hydrogel scaffolds due to its ability to produce intricate geometries which could be beneficial for cellular proliferation [7]. Nevertheless, the rheological behavior of the developed hydrogel needed to be evaluated as it can affect the printability and subsequently the stability of the scaffold [8]. Furthermore, the width of single layer filaments was used as a measurable parameter to quantify the suitability of the hydrogel for scaffold generation.

In this manner, this study presents the fabrication approach of a novel powdered biocomposite hydrogel and serves as a feasibility report for the fabrication of complex 3D scaffolds for bone tissue engineering.

2. Materials and Methods

2.1. Preparation of CS-based biocomposite

PLA (Purasorb PL 10; Purac, The Netherlands), CS, and TCP (Sigma-Aldrich, MO, USA) were cryomilled to generate powdered biocomposite. Cryogenic grinding was carried out using a freezer mill (SPEX, NJ, USA). Briefly, all the materials were weighed and transferred into a vial which was maintained at -196 ℃ using liquid nitrogen during the grinding process. The 20-minute grinding operation was divided into 4 cycles with a dwell time of 1 min between successive cycles. The composition of the generated biocomposite is as follows: 68%CS, 30%PLA and 2%TCP. The cryomilled biocomposite powders were subsequently used for the preparation of hydrogels.

2.2. Characterization of cryomilled biocomposite

X-ray diffraction (XRD) was used to confirm the occurrence of a homogenous blend of materials post-cryomilling. Rigaku Miniflex 600 XRD analysis unit (TYO, Japan) with a Cu-Kα radiation (λ = 0.154 nm) source was used with the voltage and current adjusted to 30 kV and 15 mA respectively.

Thermal characterization of the biocomposite powders was performed utilizing differential scanning calorimetry (DSC) (NETZSCH Instruments, MA, USA). Briefly, 10 mg of the sample was quenched to 10℃/min to -30℃. The sample was then heated to 190℃ followed by an isothermal step at 190 ℃ for 1 min. Another isothermal step was performed for 3 mins after cooling the samples down to -30℃. In the second heating cycle, the samples were heated to 250℃. The

glass transition temperature and melting points were analyzed using the second heating cycle to facilitate direct comparisons of the samples.

2.3. Rheological analysis of hydrogels

Three different concentrations (2.5%, 4%, and 5% w/v) of the biocomposite hydrogel were prepared using diluted acetic acid (2% v/v) (Sigma-Aldrich, MO, USA). Rheological measurements were obtained using an ARES-G2 rotational rheometer (TA Instruments, DE, USA).

Two different routines were performed to fully understand the rheological behavior of the hydrogels. The first test was a steady shear sweep test intended to study the influence of shear rate ($\dot{\gamma}$) on viscosity (η) of hydrogels. Curve fitting was then used to compute the consistency index, m ($Pa.s^n$) and power law index, n (dimensionless).

The second test was a 3-phase thixotropic test with the hydrogels being subjected to the application of shear rate periodically. The first phase lasted for 30 s with a shear rate of 0.1 s^{-1} (low), the second for 30 s with a shear rate of 200 s^{-1} (high) and the third for 60 s with a low shear rate again. The change in viscosity was plotted as a function of time and the viscosity recovery behavior of the hydrogels were analyzed. The second study was designed to resemble the actual printing process which involves the periodic application of low and high shear rates.

2.4. Single layer tests

The ideal concentration for printing the biocomposite hydrogels was identified by printing and measuring single layered scaffolds. An air pressure of 30-40 psi provided uniform extrusion of all the concentrations. The width of the extruded filaments was obtained using a microscope (Leica, IL, USA).

2.5. Scaffold fabrication

Orthogonal scaffolds (0, 90) were fabricated using a 3-axis computerized numerical control (CNC) machine (HAAS Automation, CA, USA), which was modified with the addition of a syringe head, pneumatic gauge and a controller to function as a bioplotter (Fig. 1a). The 2D sketches of the scaffolds and toolpaths were generated using Mastercam (CNC Software, CT, USA) (Fig. 1b). A pressure of ~40 psi was applied to ensure continuous deposition while a feed rate of .40 inches/min was maintained constant. The scaffolds were fabricated using an 18 G needle with a distance of .3 inches from the petri-dish. The hydrogels were dispensed into a medium containing sodium hydroxide (NaOH) (1 v/v%) (Sigma-Aldrich, MO, USA) and 100% high grade ethanol (Fischer Scientific, PIT, USA) in a 7:3 ratio.

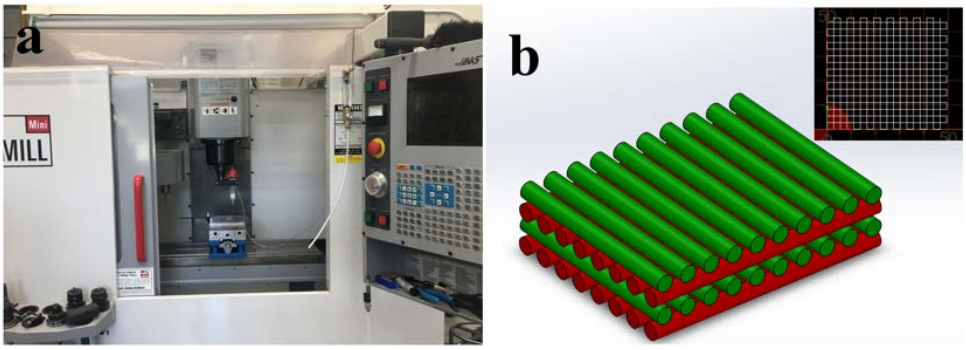

Figure 1. (a) Bioplotting set-up created by modifying a 3-axis CNC machine, (b) Schematic showing the fabricated PLA+CS+TCP filaments in 0-90 layers with the associated toolpath generated using Mastercam.

2.6. Scanning electron microscopy

Morphology of the scaffolds were studied using scanning electron microscopy (SEM) (JCM-6000Plus Neoscope JEOL, MA, USA). The pore and strand diameters were measured using JCM-600 software version 1.1. The mean diameters were calculated using thirty measurements from three independently fabricated scaffolds and represented as mean $\pm$ SD.

2.7. Short term stability analysis

In-vitro hydrolytic degradation was performed in a phosphate buffered solution (PBS) (pH=7.4) over a 14-day period. Scaffolds of 10mm x 10mm (4 layers) were immersed into a vial containing 15 ml of PBS and maintained in an incubator at 37℃. The pH values were noted down every 48 h using a pH meter (Sartorius, NY, USA).

3. Results and Discussion

3.1 X-ray diffraction

The ability of cryomilling to generate homogeneous blends of materials was confirmed using XRD. Figure 2 displays the diffractograms recorded for the as-received materials. PLA showed two distinct characteristic peaks, a strong diffraction peak at 2θ=16.38° and relatively weak peak at 2θ=18.72°. Apart from these, PLA largely exhibited the presence of amorphous regions confirming the semi-crystalline nature of the PLA used in this study. The peaks at 16.38° and 18.72° corresponded to d-spacing values of .54 nm and .47 nm which was consistent with previous studies [9]. CS showed a sharp peak at 2θ=19.44° and a relatively broad peak at 2θ=9.34° which related to d-spacing values of 0.45 nm and 0.95 nm respectively which was consistent with previously reported results [10]. TCP used in the study showed strong diffraction peaks at 2θ values of 25.66°, 31.58° and 32.68° which corresponded to d-spacing values of 0.34 nm, 0.28 nm and 0.27 nm. The peaks at 31.58° and 27.92° correspond to (0210) and (214) respectively [11]. The diffractograms of the generated biocomposite displayed both the crystalline peaks of PLA (16.38° and 18.72°) in addition to CS (19.44°) and TCP (31.58°) peaks indicating the occurrence of a homogeneous blend of the materials mixed.

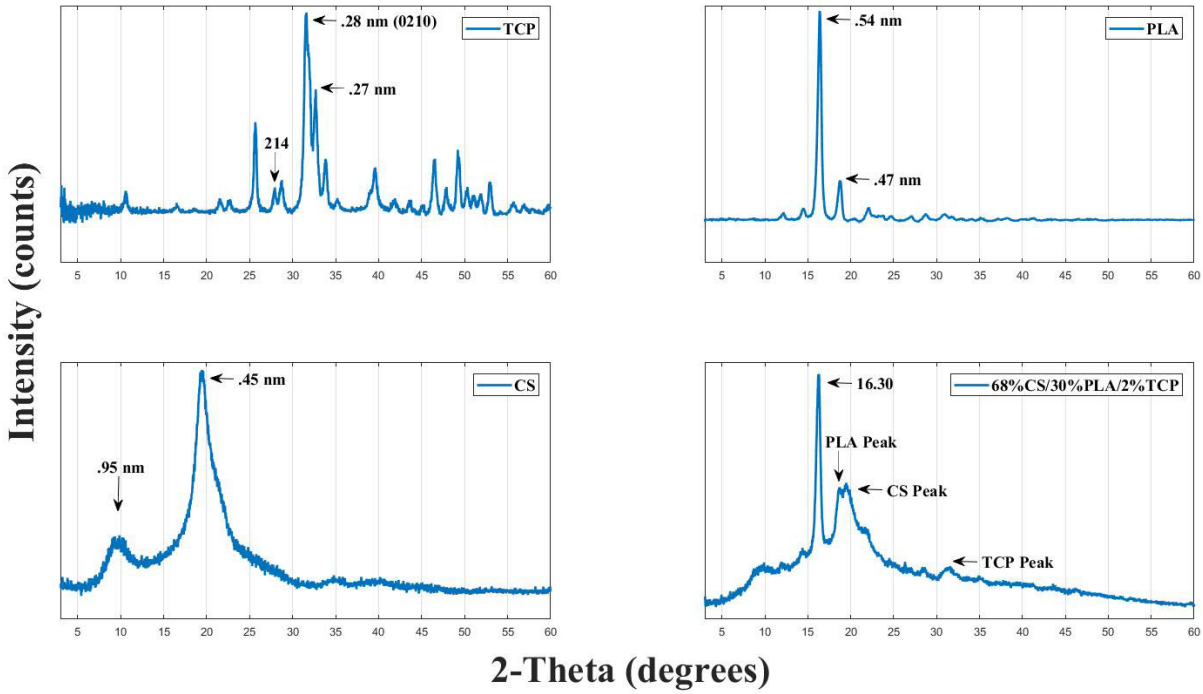

Figure 2. XRD diffractograms of the materials used in this study.

3.2. Differential scanning calorimetry

DSC was used to identify the glass transition and melting temperatures of PLA, CS and the fabricated biocomposite. The thermograms from the second heating scan are shown in Figure 3. PLA showed an average glass transition temperature of 59°C with a melting point of 178°C and an endothermic cold crystallization peak at 164°C. The melting point of CS was not observed as it is a polymer of variable length and does not display a unique melting point. The thermogram of the biocomposite showed a melting temperature (177°C) similar to that of pure PLA which indicated the formation of similar lamellae population during cold crystallization [12].

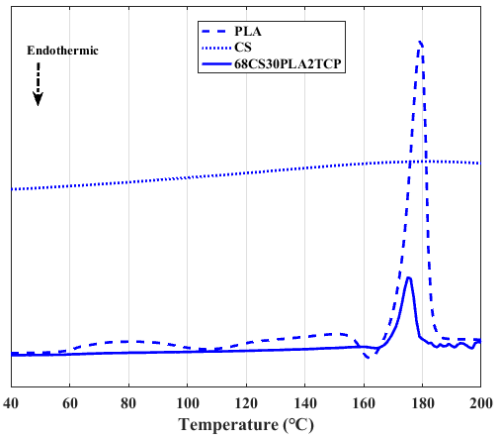

Figure 3. DSC second heating curves for PLA, CS and the cryomilled biocomposite.

3.3. Single layer tests

The single layer tests were conducted to measure the filament width as a function of material concentration. Figure 4a shows strands that were printed using 5% w/v biocomposite hydrogel and the mean strand diameter measured was 1.81±.15 mm which was greater than the diameter of the needle indicating that the hydrogel was experiencing die swell. The filament width seemed to increase with decreasing hydrogel concentration as the 4% w/v hydrogel exhibited a mean value of 1.94±.15 mm. Moreover, the 2% w/v biocomposite was unable to form individual strands due to low viscosity (Figure 4b). The results are in agreement with previously reported studies where the hydrogel with a higher concentration maintained structural integrity in comparison with the lower concentration [8].

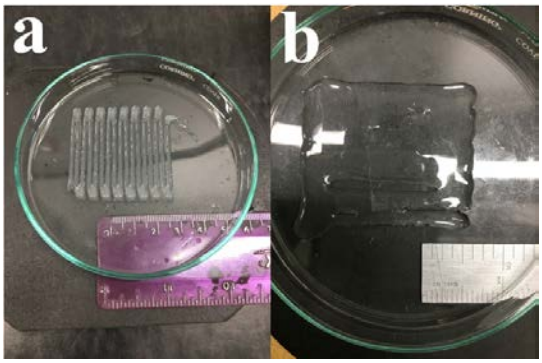

Figure 4. (a) Single layer test performed with 5% w/v composite hydrogel, (b) 2.5% w/v hydrogel displaying inability to print individual strands.

3.4. Rheological analysis

As previously mentioned, the steady shear sweep test was performed to analyze the effect of increasing shear rate on viscosity (Figure 5). The 2.5% w/v hydrogel showed a viscosity value of 5.67 Pa.s at 1 s^{-1} which dropped to 1.70 Pa.s at 100 s^{-1}. The drop in viscosity for the 4% w/v concentration was more drastic where it dropped from 30.24 Pa.s at 1 s^{-1} to 3.51 Pa.s at 100 s^{-1}. For the 5% w/v hydrogel, the viscosity dropped from 75.5 Pa.s to 2.7 Pa.s with increasing shear rate. All hydrogels exhibited typical shear thinning behavior with viscosities dropping with increasing shear rates. Based on the power law model, the constants ‘m’ and ‘n’ were obtained via curve fitting (Table 1). For a typical shear thinning liquid, the value of ‘n’ is expected to be smaller than 1 [13]. The values obtained from curve fitting clearly indicate that the higher concentration hydrogels exhibited a stronger shear thinning behavior.

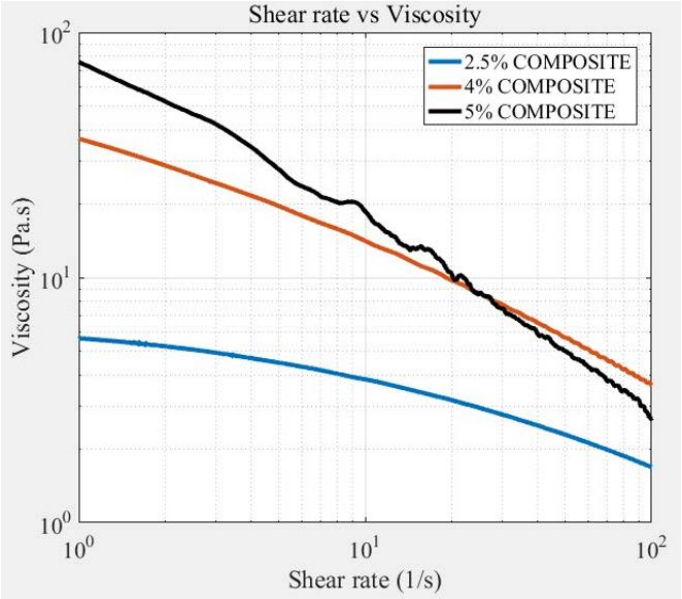

Figure 5. Viscosity of composite hydrogels as a function of shear rate at room temperature.

Table 1. 'm' and 'n' values obtained via curve fitting.

Composition (w/v)	'm' (Pa.s^n)	'n'
2.5%	6.50	.74
4%	41.85	.50
5%	87.81	.28

From a fabrication perspective, an ideal hydrogel needs to exhibit thixotropic behavior, lowering and recovering viscosities with the application and removal of shear rates. The recovery behavior of the synthesized hydrogels was analyzed using a 3-phase thixotropic test as described in section 2.3. As seen in figure 6, all the hydrogels studied exhibited considerable recovery of viscosity with the removal of shear rate. The fluctuations in the viscosity values of the 5% w/v hydrogel were explained by the reduction in the average distance between particles and an increase in particle-particle interaction and hydrodynamic effects [14]. The 5% w/v biocomposite hydrogel exhibited a slightly lower percentage of recovery (79%) when compared to the 4% w/v (86%). However, the evaluation of the aggregate results derived from filament width and rheological characteristics justify the selection of the 5% w/v biocomposite for the fabrication of scaffolds.

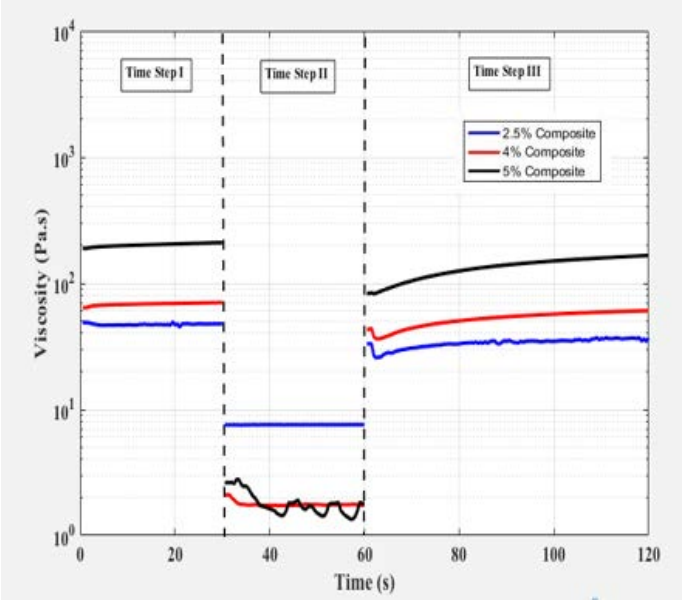

Figure 6. Viscosity as a function of time at constant shear rate for composite hydrogels.

3.5. Visual characterization

SEM was used to study the morphology of bioplotted orthogonal scaffolds. Figure 7a shows a micrograph of the fabricated biocomposite scaffold. The printed scaffolds exhibited a strand diameter of 318±30.15 μm and a pore diameter of 1131±12 μm. It was hypothesized that the presence of PLA in the scaffold would counter the effects of scaffold swelling caused by the hydrophilic chitosan. The scaffold exhibited a slightly rough texture which was seen as a positive factor that could encourage cell attachment [15]. Figure 7b shows the scaffold fabricated with 5% w/v biocomposite hydrogel.

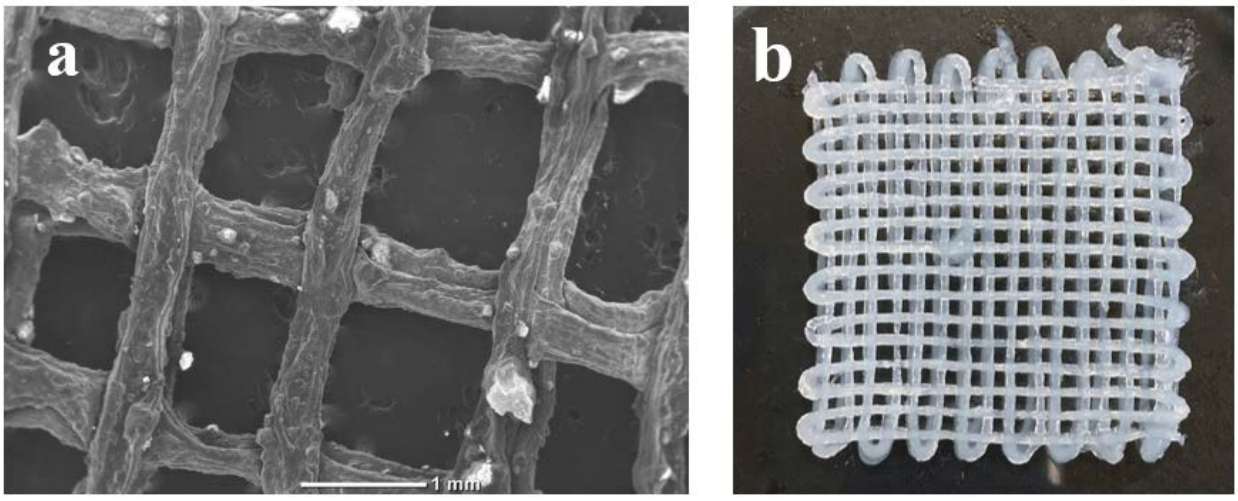

Figure 7. (a) Micrograph of the bioplotted biocomposite scaffolds (4 layers), (b) Scaffold fabricated from 5% w/v biocomposite hydrogel.

3.6. Short-term stability analysis

The short-term stability was conducted with the intention of determining the structural integrity and the degradation behavior of the scaffolds in a biological environment. To establish a control for comparison, pure chitosan scaffolds were fabricated and subjected to testing under the same conditions. The results from the pH analysis, as seen in Figure 8 indicated that the biocomposite scaffolds maintained a neutral pH while the pure chitosan scaffolds exhibited a slightly alkaline pH. It was noted that the addition of PLA can be tailored to adjust the pH of the degradation process to make it patient-friendly. In other words, the acidic degradation of PLA was able to counter the alkaline degradation of chitosan to ensure the existence of a stable neutral pH [16].

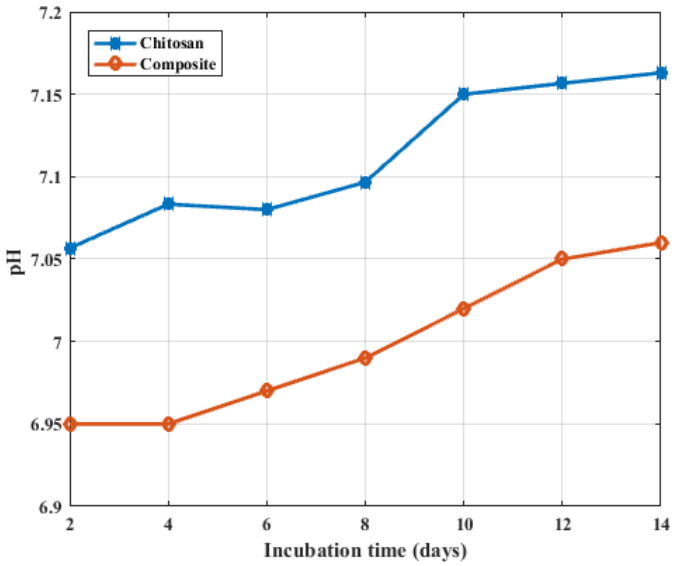

Figure 8. pH of PBS as a function of time for the fabricated scaffolds.

4. Conclusions

This study investigated the preparation and characterization of a novel biocomposite hydrogel for the fabrication of bone tissue engineering scaffolds. The rheological and filament width characterization confirmed that 5% w/v biocomposite hydrogel was the most suitable from the lot evaluated. Also, the SEM observations confirmed the production of a controlled scaffold structure. Lastly, a stable pH value was observed upon scaffold degradation which indicates the suitability of the scaffolds for implantation. Overall, the preliminary rheology studies and degradation results justify further investigation into the mechanical performance of the scaffolds along with long-term cellular response.

References

[1] T. W. Bauer and G. F. Muschler, “Bone graft materials. An overview of the basic science.,” *Clin. Orthop. Relat. Res.*, vol. 371, no. 1, pp. 10–27, 2000.

[2] C. Mason and P. Dunnill, “A brief definition of regenerative medicine,” *Regen. Med.*, vol. 3, no. 1, pp. 1–5, 2008.

[3] M. I. Sabir, X. Xu, and L. Li, “A review on biodegradable polymeric materials for bone tissue engineering applications,” *J. Mater. Sci.*, vol. 44, no. 21, pp. 5713–5724, 2009.

[4] D. W. Hutmacher, M. Sittinger, and M. V. Risbud, “Scaffold-based tissue engineering: Rationale for computer-aided design and solid free-form fabrication systems,” *Trends in Biotechnology*, vol. 22, no. 7. pp. 354–362, 2004.

[5] L. Cao *et al.*, “Degradation and osteogenic potential of a novel poly(lactic acid)/nano-sized β-tricalcium phosphate scaffold,” *Int. J. Nanomedicine*, vol. 7, pp. 5881–5888, 2012.

[6] A. J. Bavariya *et al.*, “Evaluation of biocompatibility and degradation of chitosan nanofiber membrane crosslinked with genipin,” *J. Biomed. Mater. Res. - Part B Appl. Biomater.*, vol. 102, no. 5, pp. 1084–1092, 2014.

[7] J. Suwanprateeb, W. Suvannapruk, K. Wasoontararat, K. Leelapatranurak, N. Wanumkarng, and S. Sintuwong, “Preparation and comparative study of a new porous polyethylene ocular implant using powder printing technology,” *J. Bioact. Compat. Polym.*, vol. 26, pp. 317–331, 2011.

[8] H. Li, S. Liu, and L. Lin, “Rheological study on 3D printability of alginate hydrogel and effect of graphene oxide,” *Int. J. Bioprinting*, vol. 2, no. 2, 2016.

[9] J. Ahmed, S. K. Varshney, R. Auras, and S. W. Hwang, “Thermal and rheological properties of L-polylactide/polyethylene glycol/silicate nanocomposites films,” *J. Food Sci.*, vol. 75, no. 8, 2010.

[10] C. Muzzarelli, O. Francescangeli, G. Tosi, and R. A. A. Muzzarelli, “Susceptibility of dibutyryl chitin and regenerated chitin fibres to deacylation and depolymerization by lipases,” *Carbohydr. Polym.*, vol. 56, no. 2, pp. 137–146, 2004.

[11] D. D. S. Tavares, L. D. O. Castro, G. D. D. A. Soares, G. G. Alves, and J. M. Granjeiro, “Synthesis and cytotoxicity evaluation of granular magnesium substituted β-tricalcium phosphate,” *J. Appl. Oral Sci.*, vol. 21, no. 1, pp. 37–42, 2013.

[12] V. M. Correlo, L. F. Boesel, M. Bhattacharya, J. F. Mano, N. M. Neves, and R. L. Reis, “Properties of melt processed chitosan and aliphatic polyester blends,” *Mater. Sci. Eng. A*, vol. 403, no. 1–2, pp. 57–68, 2005.

[13] R. P. Chhabra and J. F. Richardson, *Non-newtonian flow and applied rheology*. 2008.

[14] E. J. S. Duncan *et al.*, “Measurement of Fluid Rheology and Interpretation of Rheograms,” *J. Rheol. (N. Y. N. Y).*, vol. 35, no. 1, pp. 409–419, 2006.

[15] R. Murugan and S. Ramakrishna, “Development of nanocomposites for bone grafting,” *Composites Science and Technology*, vol. 65, no. 15–16 SPEC. ISS. pp. 2385–2406, 2005.

[16] J. Duan, X. Liang, Y. Cao, S. Wang, and L. Zhang, “High strength chitosan hydrogels with biocompatibility via new avenue based on constructing nanofibrous architecture,” *Macromolecules*, vol. 48, no. 8, pp. 2706–2714, 2015.